

Electrochemical and microstructural characteristics of nanoperovskite oxides $\text{Ba}_{0.2}\text{Sr}_{0.8}\text{Co}_{0.8}\text{Fe}_{0.2}\text{O}_{3-\delta}$ (BSCF) for solid oxide fuel cells

Mojgan Ahmadrzaei^{a,b}, Andanastuti Muchtar^{a,b,*}, Norhamidi Muhamad^{a,b},
C.Y. Tan^c, Edy Herianto Majlan^a

^aFuel Cell Institute, Universiti Kebangsaan Malaysia, 43600 UKM Bangi, Selangor, Malaysia

^bFaculty of Engineering & Built Environment, Universiti Kebangsaan Malaysia, 43600 UKM Bangi, Selangor, Malaysia

^cFaculty of Mechanical Engineering, University Tenaga Nasional, 43009 Kajang, Selangor, Malaysia

Received 22 April 2012; received in revised form 15 June 2012; accepted 15 June 2012

Available online 25 June 2012

Abstract

Nanoperovskite oxides, $\text{Ba}_{0.2}\text{Sr}_{0.8}\text{Co}_{0.8}\text{Fe}_{0.2}\text{O}_{3-\delta}$ (BSCF), were synthesized via the co-precipitation method using Ba, Sr, Co, and Fe nitrates as precursors. Next, half cells were fabricated by painting BSCF thin film on $\text{Sm}_{0.2}\text{Ce}_{0.8}\text{O}_x$ (samarium doped ceria, SDC) electrolyte pellets. X-ray diffraction, scanning electron microscopy (SEM), transmission electron microscopy (TEM), and electrochemical impedance spectroscopy (EIS) measurements were carried out on the BSCF powders and pellets obtained after sintering at 900 °C. Investigations revealed that single-phase perovskites with cubic structure was obtained in this study. The impedance spectra for BSCF/SDC/BSCF cells were measured to obtain the interfacial area specific resistances (ASR) at several operating temperatures. The lowest values of ASR were found to be 0.19 $\Omega\text{ cm}^2$, 0.14 $\Omega\text{ cm}^2$, 0.10 $\Omega\text{ cm}^2$, 0.09 $\Omega\text{ cm}^2$ and 0.07 $\Omega\text{ cm}^2$ at operating temperatures of 600 °C, 650 °C, 700 °C, 750 °C and 800 °C, respectively. The highest conductivity was found for cells sintered at 900 °C with an electrical conductivity of 153 S cm^{-1} in air at operating temperature of 700 °C.

© 2012 Elsevier Ltd and Techna Group S.r.l. All rights reserved.

Keywords: C: Impedance; C: Electrical conductivity; D: Perovskites; E: Fuel cells

1. Introduction

Solid oxide fuel cell is one of the most advanced types of fuel cell that maintains the highest efficiency and considered to be the most promising fuel cell used for electricity generation. However, the necessity for high operating temperatures of 800–1000 °C requires a lofty budget and present material compatibility challenges [1]. Studies show that any reduction in operating temperature reduces operating costs and expands materials selection, which

creates an opportunity for additional cost savings. Consequently, significant research has been devoted to the development of intermediate-temperature solid oxide fuel cells (IT-SOFCs) that can operate at lower temperatures of 500–800 °C. Perovskites, which are based on alkaline earth and rare earth containing cobaltites, contain materials that can serve as cathodes for SOFCs at lower temperatures [2,3] due to the fact that they offer high ionic and electronic conductivities. Lanthanum manganite LaMnO_3 , a p-type perovskite, is presently the most typical material used for cathodes. However, this works only when LaMnO_3 is used in high temperature solid oxide fuel cells. It is combined with rare earth elements such as Ba, Ce and Pr for the purpose of increasing the conductivity [4,5]. For intermediate temperature SOFCs (IT-LTSOFCs), the cathode materials must also have good electronic and ionic conductivities at temperatures below 800 °C. Recently, $\text{Ba}_x\text{Sr}_{x-1}\text{Co}_y\text{Fe}_{y-1}\text{O}_{3-\delta}$ (BSCF) materials have been reported to be very effective as cathode materials in this

*Corresponding author at: Department of Mechanical and Materials Engineering, Faculty of Engineering and Built Environment, Universiti Kebangsaan Malaysia, 43600 UKM Bangi, Selangor, Malaysia.
Tel.: +60 389216520; fax: +60 389259659.

E-mail addresses: mojgan31@gmail.com (M. Ahmadrzaei), muchtar@eng.ukm.my (A. Muchtar), hamidi@eng.ukm.my (N. Muhamad), chouyong@uniten.edu.my (C.Y. Tan), edyhm71@gmail.com (E. Herianto Majlan).

regard [6]. BSCF has a Pm3m cubic perovskite structure that exhibits high oxygen permeability and relative stability under working temperatures up to 800 °C, as well as high electrical conductivity as a result of the special arrangement of oxygen, barium, and cobalt atoms in the crystalline configuration [7]. BSCF perovskite oxides, also known as mixed ionic conductors and electrolytes (MIEC), can potentially serve as a cathode for IT-SOFC, which has high ionic conductivity [8]. At the same time, it is also potentially superior for electrochemical reduction of oxygen [7,9].

The preparation of thin electrolyte films of samarium doped ceria (SDC) with thickness of less than 100 µm has been recommended for working at low temperatures because of their higher ionic conductivity [10]. SDC is considered to be one of the most promising electrolytes for IT-SOFCs because of its superior oxygen ion conductivity and lower interfacial losses with electrodes [10,11]. In the present study, the syntheses of $\text{Ba}_x\text{Sr}_{x-1}\text{Co}_y\text{Fe}_{y-1}\text{O}_{3-\delta}$ ($x=0.2$, $y=0.8$) nanopowder of perovskite structure using the co-precipitation method is attempted. The composition, structure, morphology, grain size, area specific resistance (ASR), and conductivity of BSCF/SDC half cell were investigated where BSCF acted as a cathode and SDC was chosen as the electrolyte. In addition, the electrochemical performance of the half cell was also investigated in this work.

2. Experimental

2.1. Materials and specimen preparation

The raw materials used for the current study include $\text{Sr}(\text{NO}_3)_2$ (Sigma-Aldrich, 99%), $\text{FeCl}_2 \cdot 4\text{H}_2\text{O}$ (System, 98%), $\text{Co}(\text{NO}_3)_2 \cdot 6\text{H}_2\text{O}$ (System, 99%), $\text{Ba}(\text{NO}_3)_2$ (Merck, 99%), HCl (Merck, 37%), $(\text{NH}_4)_2\text{C}_2\text{O}_4 \cdot \text{H}_2\text{O}$ (Merck, 99%), $\text{Sm}_{0.2}\text{Ce}_{0.8}\text{O}_x$ (Sigma-Aldrich, 99%), Ethyl cellulose (Sigma-Aldrich), $\text{C}_{10}\text{H}_{18}\text{O}$ (Merck, 90%), and NH_4OH (Merck, 25% NH_3 in H_2O). Nanostructured $\text{Ba}_{0.2}\text{Sr}_{0.8}\text{Co}_{0.8}\text{Fe}_{0.2}\text{O}_{3-\delta}$ (BSCF) were synthesized using the oxalate co-precipitation method. First, all the metal ions were dissolved in distilled water, prior to mixing with the proper amount of ammonium oxalate. The pH value was 2–3 with the aid of ammonia and hydrochloric acid [12]. The precipitate was dried in an oven at 110 °C for 2 h. Finally, the dried precipitate was calcined at 900 °C to obtain BSCF.

The SDC powder was calcined at 700 °C for 2 h with a heating rate of 2 °C/min to remove any remaining carbon residues in the powder. Subsequently, the SDC powder was cold pressed at 150 MPa into cylindrical pellets (13 mm in diameter and 2 mm in thickness). The SDC pellets were then sintered at 1350 °C for 5 h with a heating rate of 3 °C/min.

Initially, BSCF powder (70 wt%) was mixed with a binder (ethyl cellulose, 5 wt%) and solvent (terpineol 25 wt%). The slurry was then inserted into the ball mill

tool comprising a zirconia bowl with zirconia balls, which were grinding at 100 rpm for 12 h, for spinning to obtain a more homogeneous and fine slurry. The resulting slurry was later painted on the SDC electrolyte to form a half-cell. Subsequently, the half-cell of BSCF/SDC/BSCF was dried and fire-dwelled at 500 °C for 2 h at a heating rate of 2 °C/min to remove the organics, and then sintered at 900 °C for 1 h at a heating rate of 2 °C/min.

2.2. Characterization methods

The crystal structure of the powder was analyzed via X-ray powder diffraction (Bruker D8 Advance) with $\text{Cu-K}\alpha$ radiation at an operating voltage and current of 60 kV and 60 mA, respectively. The morphology of the powder and the films were examined using a Zeiss Supra-55VP field emission scanning electron microscopy (FESEM) and transmission electron microscopy (TEM). Impedances of symmetrical cells were measured using Solarton SI 1286 and a High Frequency Response Analyzer (HFRA). The analysis was performed by applying a frequency of 10–100 kHz, with an alternating current of 100 mV. The analysis was performed at a temperature of 500–800 °C with temperature intervals of 50 °C in air. The experiment arrangement is schematically shown in Fig. 1.

3. Results and discussion

3.1. XRD analysis

The XRD pattern of BSCF powder after calcination at 900 °C is shown in Fig. 2. All the observed peaks for the sample calcined at 900 °C for 2 h were properly indexed as a cubic perovskite structure without miscellaneous peaks of secondary phases. Comparable results were observed in previous studies [13–16]. All the peaks have been properly indexed and indicated the formation with a space group of Pm3m (221) and cubic perovskite (01-0756980) structure [17,18].

3.2. Particle size and microstructure analysis

The optimization of the microstructure is important for the best fuel cell performance. One aspect that should be considered in optimizing the microstructure of the cathode is the calcination temperature [19]. In addition, the rate of charge transfer is usually highly related to the microstructure, such as the particle size and the compositional homogeneity of cathode. The FESEM micrograph in Fig. 3 shows the morphology of powders obtained in the current work, which were calcined at 900 °C. The results of the particle size analysis indicate that the BSCF powder has a small particle size of 40 nm and compositional homogeneity has been achieved, as well as structural uniformity. Meanwhile, Xueli [20] stated that their BSCF powder of a slightly different composition of

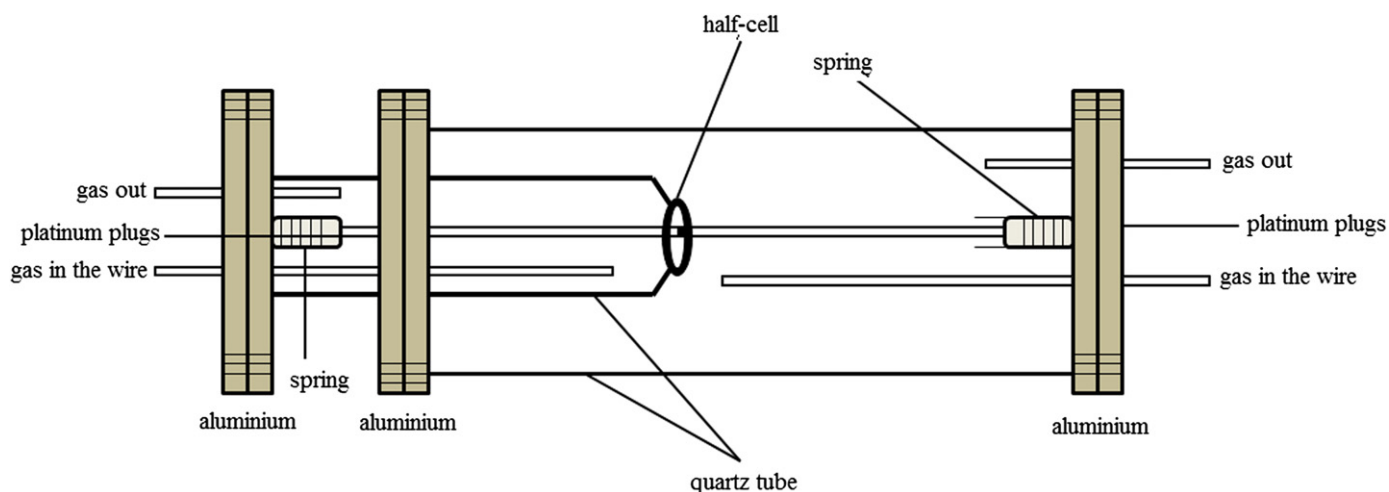


Fig. 1. Schematics of the cell electrochemical impedance spectroscopy.

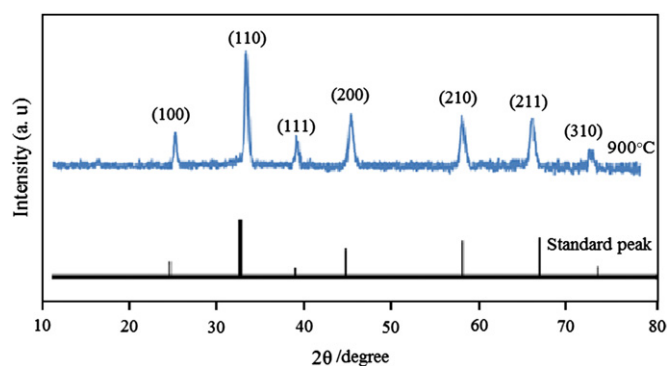


Fig. 2. XRD patterns of BSCF powder calcined at 900 °C.

$\text{Ba}_{0.5}\text{Sr}_{0.5}\text{Co}_{0.2}\text{Fe}_{0.8}\text{O}_{3-\delta}$ obtained via citrate method has a particle size between 1 μm and 2 μm , which is much larger than the BSCF prepared in the current study. Another BSCF powder of composition $\text{Ba}_{0.5}\text{Sr}_{0.5}\text{Co}_{0.8}\text{Fe}_{0.2}\text{O}_{3-\delta}$ generated by the combined EDTA–citrate complexing method was found to produce a particle size between 6.9 μm and 9.3 μm [21], which is also greater than the BSCF powder generated in the current study. The difference between the sizes of the particles produced in the present study with previous studies show that the production method and the calcination temperature have significant impact on the size of the powder particles and its compositional homogeneity.

The energy-dispersive X-ray (EDX) method was used to verify the compositional homogeneity and structural uniformity. The EDX data for several selected different parts showed that the co-precipitation method resulted in the most homogeneous elemental concentration of perovskite materials.

The particle size is further analyzed via transmission electron microscopy (TEM). Fig. 4 shows the BSCF nanopowder calcined at 900 °C composed of uniform particles. The initially formed precursor nanoparticles were reduced in size from chemical grinding of the precursors

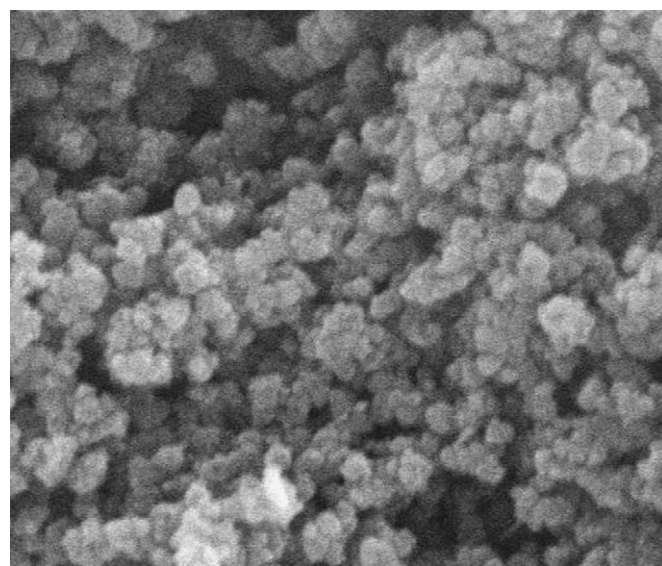


Fig. 3. SEM micrograph of BSCF powder calcined at 900 °C.

which will form the desired perovskite phase. Very uniform particle size distribution and compositional homogeneity are achieved by the co-precipitation method for the particles with a mean size of 40 nm.

3.3. Area specific resistance (ASR)

The typical impedance spectra for BSCF as SOFC cathode with SDC as electrolyte that were measured under air atmosphere at 600–800 °C are shown in Fig. 5(a). Results show that the resistances decrease with increasing temperature from 600 °C to 700 °C after which the resistances again increased at 750 °C and 800 °C. The impedance curve reflects the processes that control the oxygen reduction at the cathode BSCF after 700 °C, in which the resistances were increased because the charged oxygen vacancy mechanism is outweighed by the formation of

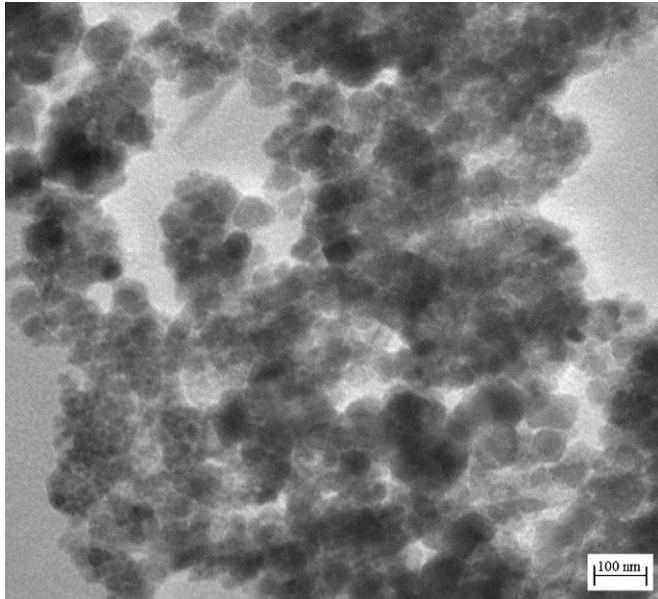


Fig. 4. TEM image of BSCF calcined at 900 °C.

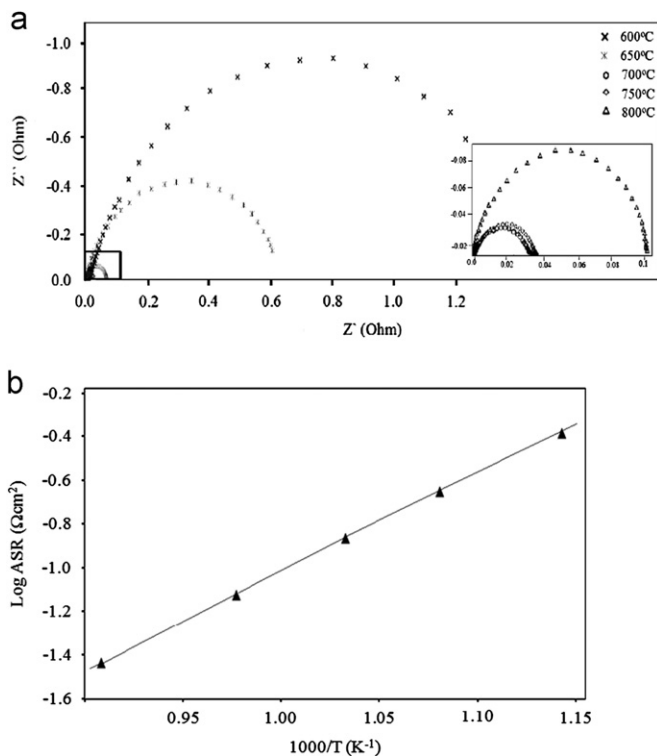


Fig. 5. Electrochemical impedance of BSCF at different operating temperatures (a) and the temperature dependence of area specific resistance (ASR) of the BSCF cathode (b).

oxygen vacancies. This phenomenon is common in BSCF crystals [22].

Cell impedance spectroscopy analysis was then carried out to determine the electrochemical properties, such as area specific resistance (ASR) and conductivity. The ASR values of BSCF are determined from the corresponding impedance spectra and are shown in Fig. 5(b). ASR is large

at lower operating temperatures. The ASR value decreases with increasing operating temperature (in particular above 700 °C). The lowest values for the ASR at operating temperatures of 600 °C, 650 °C, 700 °C, 750 °C and 800 °C were found to be $0.19 \Omega\text{cm}^2$, $0.14 \Omega\text{cm}^2$, $0.10 \Omega\text{cm}^2$, $0.09 \Omega\text{cm}^2$ and $0.07 \Omega\text{cm}^2$, respectively. The study shows that the microstructure of the BSCF cathode greatly influences the specific resistance of the cathode area. A good fuel cell has a value of $\text{ASR} < 0.1 \Omega\text{cm}^2$ [23]. Therefore, the BSCF cathode in the present study has shown favorable performance for operating temperatures of 700 °C and higher.

3.4. Electrochemical analysis

The overall electrical conductivity consists of ionic conductivity and electronic conductivity, which were measured using impedance spectroscopy. In the BSCF cathode, the electronic conductivity is created via the transition of Co, Fe cations between the triple and the tetravalent states. At low temperatures, Fe^{4+} , Co^{4+} , Ba^{+3} , and Sr^{+3} exist in a compound. The concentration of oxygen ions also increases when the operating temperature increases, mainly because of the release of lattice oxygen. This condition in turn promotes the thermal reduction of Fe, Co, Ba, and Sr cations to lower valence states, leading to the increase in electrical conductivity [22]. The conduction mechanism of oxide BSCF perovskite can be described as the following redox reactions:



Therefore, the electrical conductivity measured in the current study can be considered to refer only to the electronic conductivity, because the oxide ion conductivity of BSCF perovskite is twice as low as the electronic conductivity [24]. Fig. 6 shows the electrical conductivity measurements and comparison of the specific conductivity of nanostructured synthesized $\text{Ba}_x\text{Sr}_{x-1}\text{Co}_y\text{Fe}_{y-1}\text{O}_{3-\delta}$ ($x=0.5$, $y=0.8$) [25], and conventional $\text{Ba}_x\text{Sr}_{x-1}\text{Co}_y\text{Fe}_{y-1}\text{O}_{3-\delta}$ ($x=0.5$, $y=0.5$ without nanostructure) [26], as well as the nanostructured $\text{Ba}_x\text{Sr}_{x-1}\text{Co}_y\text{Fe}_{y-1}\text{O}_{3-\delta}$ ($x=0.2$, $y=0.8$) in the current study. All samples show that the pattern of the BSCF conductivity is similar in that it increases with increasing temperature until the operating temperature reaches 700 °C.

The conductivity of the highest possible BSCF at a temperature of 700 °C followed other compositions of a similar product. The BSCF oxide series is able to provide high electrical conductivity owing largely to the presence of the valent-alterable Co and Fe cations. This phenomenon is due to the high Sr content and substitution of Co or Fe with Sr cations with relative lower ionic value state (+3). Such a condition will lead to the increase in oxygen

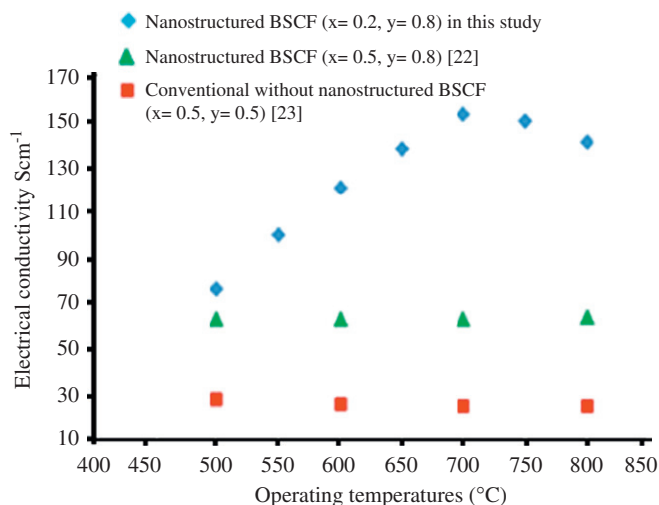


Fig. 6. Electrical conductivity of the BSCF cathode as prepared in this study at operating temperatures of 500–800 °C compared with others from earlier published works.

vacancy concentration in the BSCF samples, resulting in increased electrical conductivity [26]. In addition, at around 700 °C, the proportion between the number of triple and tetravalent state cations reaches an optimum value. This yields the highest concentration of electron holes, thus leading to the highest electrical conductivity. However, after the operating temperature increases, the number of Fe^{3+} , Co^{3+} , Ba^{+2} and Sr^{+2} cations in the perovskite is greater than required, leading to the undesired decrease in the concentration of electrons. Consequently, the total electrical conductivity will be reduced. Nevertheless, the BSCF samples in this study have shown to provide sufficiently high conductivity and potentially able to serve as a cathode for IT-SOFCs (153 S cm^{-1} at 700 °C).

4. Conclusion

$\text{Ba}_{0.2}\text{Sr}_{0.8}\text{Co}_{0.8}\text{Fe}_{0.2}\text{O}_{3-\delta}$ (BSCF) powder has been successfully produced via the co-precipitation method. The process is called chemical grinding because the decomposition of the precursor forms the desired perovskite phase. Using X-ray diffraction techniques, the BSCF was confirmed to be single phase with pure cubic structure. The results of the current study show that 900 °C is a suitable calcination temperature with small particle size of less than 40 nm. The corresponding ASR values measured were $0.19 \Omega \text{ cm}^2$ at 600 °C, $0.14 \Omega \text{ cm}^2$ at 650 °C, $0.10 \Omega \text{ cm}^2$ at 700 °C, $0.09 \Omega \text{ cm}^2$ at 750 °C and $0.07 \Omega \text{ cm}^2$ at 800 °C, respectively. BSCF exhibited the highest conductivity at a temperature 700 °C (153 S cm^{-1}).

Acknowledgments

The authors would like to acknowledge Universiti Kebangsaan Malaysia and the Malaysian Government

for research sponsorship under the Arus Perdana Grant project funding UKM-TK-AP-05-09 and UKM-AP-TK-08-2010.

References

- [1] X. Meng, B. Meng, X. Tan, N. Yang, Z.F. Ma, Synthesis and properties of $\text{Ba}_{0.5}\text{Sr}_{0.5}(\text{Co}_{0.6}\text{Zr}_{0.2})\text{Fe}_{0.2}\text{O}_{3-\delta}$ perovskite cathode material for intermediate temperature solid-oxide fuel cells, *Materials Research Bulletin* 44 (2009) 1293–1297.
- [2] V. Huang, J.B. Goodenough, A solid oxide fuel cell based on Sr- and Mg doped LaGaO_3 electrolyte: the role of a rare-earth oxide buffer, *Alloys and Compounds* 303 (304) (2000) 454.
- [3] J. Liu, B.D. Madsen, Z. Ji, S.A. Barnett, Fuel-flexible ceramic-based anode for solid oxide fuel cells, *Electrochemical and Solid-State Letters* 5 (2002) A122–A124.
- [4] C.O. Augustin, L.J. Berchmans, R.K. Selvan, Structural, electrical and electrochemical properties of co-precipitated $\text{SrFeO}_{3-\delta}$, *Journal of Materials Letters* 58 (2004) 1260–1266.
- [5] X. Meng, B. Meng, X. Tan, N. Yang, Z.F. Ma, Synthesis and properties of $\text{Ba}_{0.5}\text{Sr}_{0.5}(\text{Co}_{0.6}\text{Zr}_{0.2})\text{Fe}_{0.2}\text{O}_{3-\delta}$ perovskite cathode material for intermediate temperature solid-oxide fuel cells, *Materials Research Bulletin* 44 (2009) 1293–1297.
- [6] W. Zhou, R. Ran, Z. Shao, Progress in understanding and development of $\text{Ba}_{0.5}\text{Sr}_{0.5}\text{Co}_{0.8}\text{Fe}_{0.2}\text{O}_{3-\delta}$ based cathodes for intermediate-temperature solid-oxide fuel cells, *Power Sources* 192 (2009) 231–246.
- [7] J. Raharjo, A. Muchtar, W.R.W. Daud, N. Muhamad, E.H. Majlan, Fabrication of dense composite ceramic electrolyte $\text{SDC}(\text{Li}/\text{Na})_2\text{CO}_3$, *Key Engineering Materials* 447 (448) (2010) 666–670.
- [8] H. Zhao, L. Huo, L. Sun, L. Yu, S. Gao, J. Zhao, Preparation, chemical stability and electrochemical properties of LSCF-CBO composite cathodes, *Material Chemistry and Physics* 88 (2004) 160–166.
- [9] V. Dusastre, J.A. Kilner, Properties of pyrochlore ruthenate cathodes for intermediate temperature solid oxide fuel cells, *Solid State Ionics* 122 (1999) 41–49.
- [10] G.A. Tompsett, N.M. Sammes, J. Am, Ceria-Yttria stabilized composite systems for application as low temperature electrolytes, *Ceramic Society* 80 (1997) 3181–3186.
- [11] K. Zheng, B.C.H. Steele, T. Kawada, I.S. Metcalfe, Solid oxide fuel cells based on $\text{Ce}(\text{Gd})\text{O}_{2-x}$ electrolytes, *Solid State Ionics* 86–88 (1996) 1241–1244.
- [12] J. Peña-Martínez, D. Marrero-López, J.C. Ruiz-Morales, P. Núñez, C. Sánchez-Bautista, A.J. Dos Santos-García, J. Canales-Vázquez, On $\text{Ba}_{0.5}\text{Sr}_{0.5}\text{Co}_{1-y}\text{Fe}_y\text{O}_{3-\delta}$ ($y=0.1-0.9$) oxides as cathode materials for $\text{La}_{0.9}\text{Sr}_{0.1}\text{Ga}_{0.8}\text{Mg}_{0.2}\text{O}_{2.85}$ based IT-SOFCs, *Hydrogen Energy* 34 (2009) 349486–349495.
- [13] V. Guidi, M.A. Butturi, M.C. Carotta, B. Cavicchi, M. Ferroni, C. Malagù, G. Martinelli, D. Vincenzi, M. Sacerdoti, M. Zen, Gas sensing through thick film technology, *Sensors and Actuators B* 84 (2002) 72–77.
- [14] M. Lee, T. Lin, C. Wang, Y. Chang, Fabrication and characterization of a $\text{Ba}_{0.5}\text{Sr}_{0.5}\text{Co}_{0.8}\text{Fe}_{0.2}\text{O}_{3-\delta}$ Gadolinia-doped ceria cathode for an anode-supported solid-oxide fuel cell, *Power Sources* 195 (2010) 2220–2223.
- [15] S. Švarcová, K. Wiik, J. Tolchard, H.J.M. Bouwmeester, T. Grande, Structural instability of cubic perovskite $\text{Ba}_x\text{Sr}_{1-x}\text{Co}_{1-y}\text{Fe}_y\text{O}_{3-\delta}$, *Solid State Ionics* 178 (2008) 1787–1791.
- [16] M. Ahmadrezaei, A. Muchtar, N. Muhamad, C.Y. Tan, Preparation and evaluation of $\text{Ba}_x\text{Sr}_{(x-1)}\text{Co}_y\text{Fe}_{(y-1)}\text{O}_{3-\delta}$ nanomaterial for SOFC cathode by oxalate co-precipitation ($x=0.2$, $y=0.8$), *Applied Mechanics and Materials* 52–54 (2011) 1177–1181.
- [17] W. Zhou, R. Ran, Z. Shao, Progress in understanding and development of $\text{Ba}_{0.5}\text{Sr}_{0.5}\text{Co}_{0.8}\text{Fe}_{0.2}\text{O}_{3-\delta}$ based cathodes for intermediate-temperature solid-oxide fuel cells, *Power Sources* 192 (2009) 231–246.
- [18] P. Zeng, R. Ran, Z. Chen, H. Gu, Z. Shao, J.A. Diniz da Costa, S. Liu, Significant effects of sintering temperature on the

- performance of $\text{La}_{0.6}\text{Sr}_{0.4}\text{Co}_{0.2}\text{Fe}_{0.5}\text{O}_{3-\delta}$ oxygen selective membranes, *Membrane Science* 302 (2007) 171–179.
- [19] H.A. Rahman, A. Muchtar, N. Muhamad, H. Abdullah, Electro-phoretic deposition of $\text{La}_{0.6}\text{Sr}_{0.4}\text{Co}_{0.2}\text{Fe}_{0.8}\text{O}_{3-\delta}$ TM cathode film on stainless steel substrates, *Advanced Materials Research* 139–14 (2010) 145–148.
- [20] Q. Xueli, D. Huang, F. Zhang, W. Chen, M. Chen, H.X. Liu, Structure, electrical conducting and thermal expansion properties $\text{La}_{0.6}\text{Sr}_{0.4}\text{Co}_{0.8}\text{Fe}_{0.2}\text{O}_{3-\delta}$ – $\text{Ce}_{0.8}\text{Sm}_{0.2}\text{O}_{2-\delta}$ composite cathodes, *Journal of Alloys and Compounds* 454 (2007) 460–465.
- [21] I.M. Hung, C.Y. Liang, C.J. Ciou, R.Z. Song, Z.Y. Lai, Effect of pH value on the synthesis and characterization of $\text{Ba}_{0.5}\text{Sr}_{0.5}\text{Co}_{0.8}\text{Fe}_{0.2}\text{O}_{3-\delta}$ powders prepared by the citrate–EDTA complexing method, *Journal of Materials Science* 45 (2010) 3824–3832.
- [22] S. Wang, M. Katsuki, M. Dokiya, T. Hashimoto, High temperature properties of $\text{La}_{0.6}\text{Sr}_{0.4}\text{Co}_{0.5}\text{Fe}_{0.2}\text{O}_{3-\delta}$ phase structure and electrical conductivity, *Journal of Solid State Ionics* 159 (2003) 71–78.
- [23] V. Dusastre, J.A. Kilner, Properties of pyrochlore ruthenate cathodes for intermediate temperature solid oxide fuel cells, *Journal of Solid State Ionics* 122 (1999) 41–49.
- [24] D.J. Chen, R. Ran, K. Zhang, J. Wang, Z.P. Shao, Intermediate-temperature electrochemical performance of a polycrystalline $\text{PrBaCo}_2\text{O}^{5+\delta}$ cathode on samarium-doped ceria electrolyte, *Power Sources* 188 (2008) 96–105.
- [25] M. Darab, M.S. Toprak, G.E. Syvertsen, M. Muhammed, Nanoengineered BSCF cathode materials for intermediate-temperature solid-oxide fuel cells, *Journal of Electrochemical Society* 156 (2009) K139–K143.
- [26] B. Wei, Z. Lü, S.Y. Li, Y.Q. Liu, K. Liu, W.H. Su, Thermal and electrical properties of new cathode material $\text{Ba}_{0.5}\text{Sr}_{0.5}\text{Co}_{0.8}\text{Fe}_{0.2}\text{O}_{3-\delta}$ for solid oxide fuel cells, *Electrochemical and Solid-State Letters* 8 (2005) A428–A431.